Mem. Natl Inst. Polar Res., Spec. Issue, **56**, 287–294, 2002

# The effect of hydrostatic pressure on crack formation in ice single crystals

Atsushi Miyamoto, Hitoshi Shoji and Kinji Hyakutake

*Kitami Institute of Technology, 165, Koencho, Kitami 090-8507*

***Abstract:*** Many tiny cracks are observed near the surface of deep ice cores drilled from polar ice sheets. These cracks probably form during the ice core drilling process at hydrostatic pressure, which increases linearly with depth. We studied crack formation in ice experimentally by deforming ice single crystals using a uniaxial compression apparatus with controlled hydrostatic pressure. The uniaxial compressive stress was applied to ice samples under a hydrostatic pressure of 20 MPa at $-18$°C. A constant strain rate was set at $\sim 10^{-7}$ s$^{-1}$. The *c*-axis orientations of the ice single crystals were parallel to the compression axis. The compression test results show that cracks formed in ice samples at a stress level of over 15 MPa after 0.5% compressive strain, except for samples that deformed non-uniformly. These cracks grew along basal and parallel planes to the *c*-axis. This result suggests that the tiny cracks at the surface of ice cores could originate in local high stress just under the tip of the cutter.

## 1. Introduction

Analysis of bubbles in ice cores is a technique by which one can directly examine ancient air. But, because retrieval of deep ice cores is very difficult, only a few deep ice cores exist, from Antarctica and Greenland. Detailed analysis becomes possible only by recovering high-quality ice cores—the physical and chemical signals in ice cores are deteriorated by cracks. In fact, many tiny cracks are observed near the surface of deep ice cores immediately after being drilled from polar ice sheets (Fig. 1). Additionally, in a laboratory drill test, the formation of many tiny cracks has been observed under the tip of the cutter (Y. Fujii and Y. Tanaka, pers. commun.). To improve the analyses, it is important to recover crack-free ice cores.

In this study, the strength of ice and crack formation under hydrostatic pressure are discussed as they apply to deep ice core drilling. To learn how to obtain crack-free ice cores, we measured the strength and conditions for crack formation in ice single crystals by carrying out a uniaxial compression test under ambient pressure and hydrostatic pressure. We use ice single crystals to obtain fundamental information on crack formation in ice. Although the mechanical properties of ice single crystals have been studied previously (*i.e.* Nakaya, 1958; Higashi *et al.*, 1964; Jones and Glen, 1969; Jones and Brunet, 1978) there are no previous mechanical tests on ice single crystals loaded parallel to the *c*-axis. This is because there is no resolved shear stress on the basal or prism plane of ice single crystals in this arrangement. In our experiments, the stress axis was set parallel to the *c*-axis to more easily compare to the drilling of strongly anisotropically-textured ice that typically

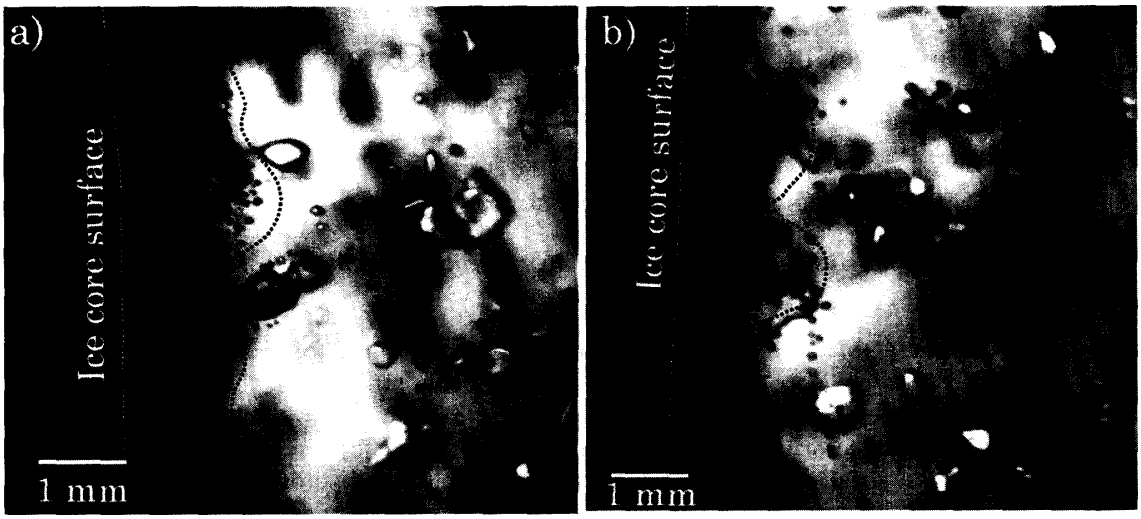


*Fig. 1. Cracks on the surface of the GRIP ice core at a) 1328 m, and b) 1548 m. The original shape of each crack is preserved as a collection of many small bubbles. These photographs were taken along the core axis and thus show cross-sections normal to the core axis.*

exhibits single maximum fabrics at this orientation in deep parts of ice sheets.

## 2. Experimental

Our ice single crystal was made from ultrapure water by using a crystal pulling method. It contained no bubbles. Test samples were cut from this ice single crystal. The samples had rectangular cross-sections between 2 and 8 $cm^2$ with lengths between 3 and 9 cm. The long axes of these rectangular samples were along the *c*-axis orientation. The *c*-axis orientation of the single crystal, and therefore of each sample, was determined using a universal stage. Uniaxial compression tests were carried out using the JACOM model JTS-3010 apparatus, which could be kept at 70 MPa maximum inner hydrostatic pressure (Fig. 2). The uniaxial compression sample was set in a pressure chamber filled with silicone oil. The bottom of the test sample was fixed on the apparatus platen. The top of the test sample was not fixed on the upper apparatus platen. Hydrostatic pressure was applied to the pressure chamber at 20 MPa by a hydraulic pump. The load, displacement, temperature, and pressure were controlled by the control system. The experimental temperature was kept at $-18°C$ during each test run, and a constant strain rate was maintained for each sample at about $10^{-7}\ s^{-1}$. Before the compression test, the hydrostatic pressure in the pressure chamber was increased to 20 MPa at a rate of 10 to 20 MPa/hour; the pressure was decreased to ambient pressure at a rate of 5 to 20 MPa/hour after the compression test.

## 3. Results and discussion

No visible cracks formed in the bubble-free, single crystal samples when the hydrostatic pressure was raised at 20 MPa/hour from ambient pressure up to 20 MPa, then lowered back to ambient pressure at the same rate. All experimental conditions and

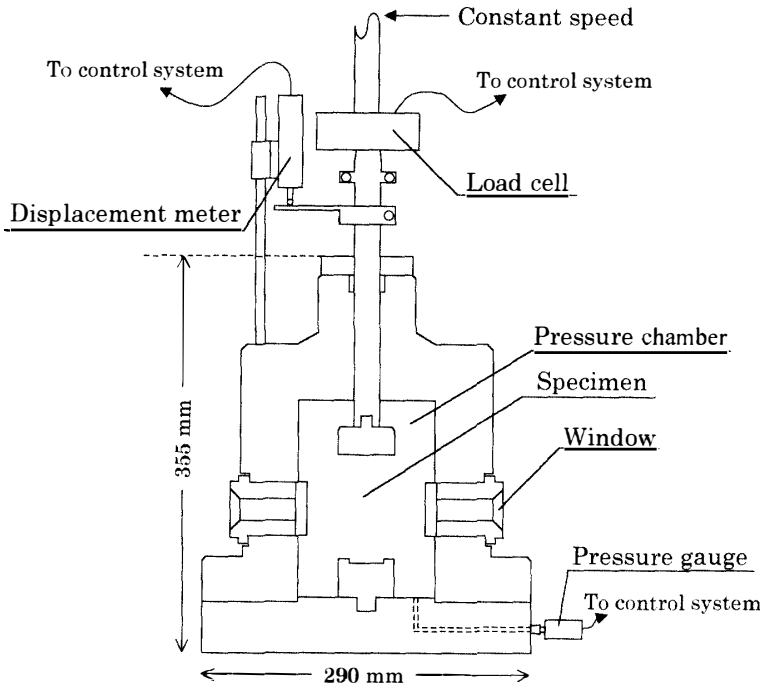


*Fig. 2. Schematic of the uniaxial compression test apparatus.*

results are shown in Table 1. Figures 3 and 4 show the stress-strain curves. The stress-strain curve of No. 12 was not available, because of a control system error. Figure 3 shows the stress-strain curves for the samples that did not crack. When no crack formed, the maximum stress levels were less than 15 MPa except for samples No. 5 and 8. Recrystall-

*Table 1. Conditions and results of uniaxial compression tests.*

| Sample No. | Sample size: Height, mm | Sample size: Cross section, $cm^2$ | Hydrostatic pressure, MPa | Temperature, °C | Strain rate, $\times 10^{-7}$ $s^{-1}$ | Total strain, % | Stress, MPa | Crack type |
|---|---|---|---|---|---|---|---|---|
| 1 | 93.35 | 8.02 | 0.1 | −18 | 0.9 | 4.83 | 13.4 | 1 |
| 2 | 87.90 | 5.71 | 20.0 | −18 | 0.9 | 3.03 | 9.8 | 1 |
| 3 | 59.65 | 7.16 | 20.0 | −18 | 1.4 | 0.55 | 18.3 | 2b |
| 4 | 58.80 | 5.04 | 20.0 | −18 | 1.4 | 0.47 | 26.1 | 2b |
| 5 | 52.25 | 4.39 | 20.0 | −18 | 1.6 | 5.07 | 24.8 | 1 |
| 6 | 34.45 | 1.89 | 20.0 | −18 | 2.4 | 4.24 | 12.8 | 1 |
| 7 | 36.55 | 2.59 | 20.0 | −18 | 2.3 | 7.15 | 13.9 | 1 |
| 8 | 29.85 | 3.05 | 20.0 | −18 | 2.8 | 8.58 | 22.5 | 1 |
| 9 | 67.35 | 6.42 | 0.1 | −18 | 1.2 | 3.40 | 28.1 | 2a |
| 10 | 59.00 | 6.49 | 0.1 | −18 | 1.4 | 5.11 | 27.6 | 2a |
| 11 | 26.00 | 5.03 | 20.0 | −18 | 3.2 | 1.35 | 26.0 | 2b |
| 12 | 26.75 | 4.87 | 0.1 | −18 | 3.1 | 5.98 | 22.5 | 2a |

Note: In the crack type column, **1** indicates no crack formation; **2a** indicates cracks grew along parallel plane to the *c*-axis; **2b** indicates cracks grew mostly along basal plane.

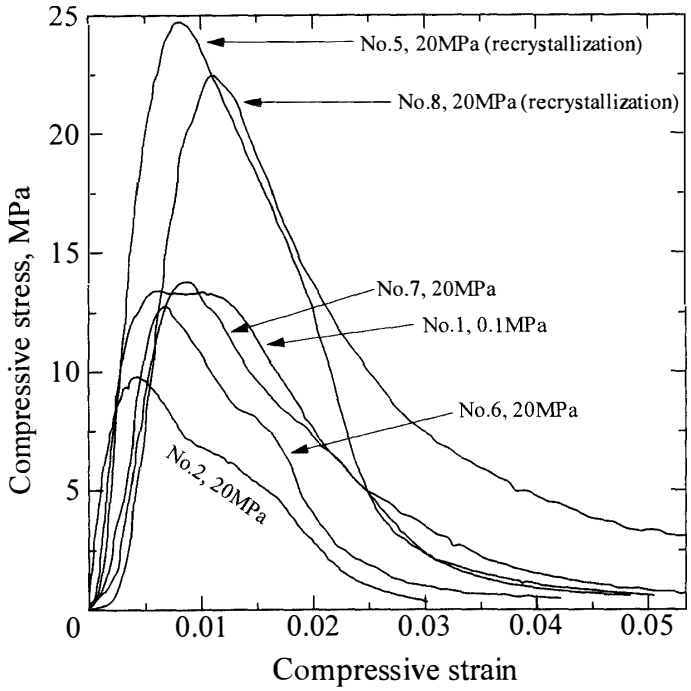


*Fig. 3. Stress-strain curves of the samples that did not crack. The number of the sample and the applied hydrostatic pressure are shown next to each curve.*

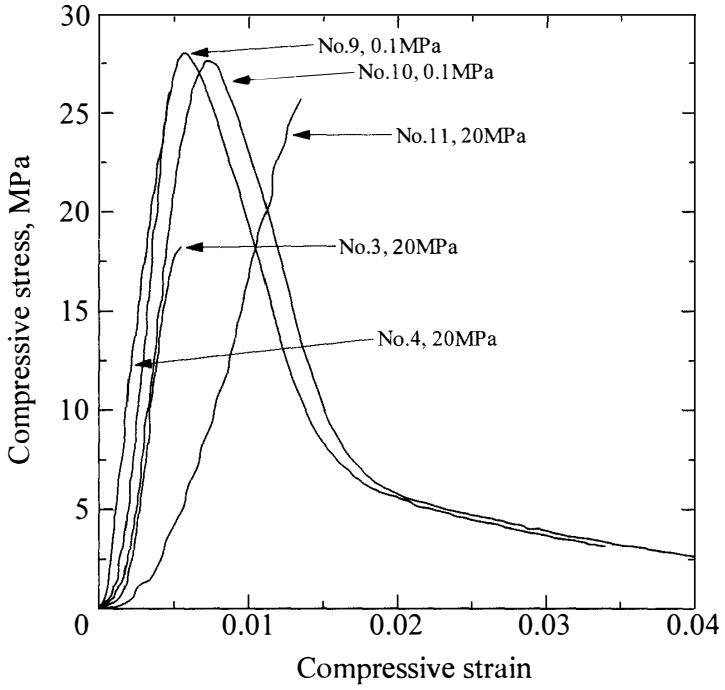


*Fig. 4. Stress-strain curves of the samples that cracked. The number of the sample and the applied hydrostatic pressure are shown next to each curve.*

ized grains were observed in samples No. 5 and 8 after the compression test. Therefore, we do not directly compare them with the other samples. Figure 4 shows stress-strain curves for the samples that cracked; the maximum stress levels of all these samples were over 15 MPa. Under both ambient pressure and hydrostatic pressure, cracks grew along either a basal and/or parallel plane to the *c*-axis. These cracks had already been observed to form during the compression tests. The result of each mechanical test was classified into one of the following two types depending on whether or not cracks formed. The type number (1, 2a, 2b) is shown in Table 1.

1) No cracks formed in the compression samples. These samples deformed non-uniformly with bending and twisting (Fig. 5a) under both experimental conditions of ambient pressure and hydrostatic pressure. This bending begins with a few discrepancies of the misorientation angle between the stress axis and *c*-axis of the sample during experimental preparation. Once bending begins, the deformation proceeds at a stress level of less than 15 MPa without crack formation. The angle between the stress axis and sample *c*-axis was larger than that at test commencement. No resolved shear stress is applied along the basal plane near the bending; therefore, the sample can be deformed at a lower stress level by basal gliding. In sample No. 2 (Fig. 5a), twisting was observed in addition to bending. The bending deformation is similar to the situation described in the three-point bending test by Nakaya (1958).

2a) Cracks grew mostly along the plane parallel to the *c*-axis (Fig. 6a), but some small cracks grew along basal planes in sample No. 10. This was observed only in the ambient pressure experiment. These cracks appear by expanding horizontally away from the *c*-axis (Fig. 6b) and the vertical strain is caused by barreling. Trickett *et al.* (2000) conducted a constant strain rate compressive test on ice single crystals with a wide

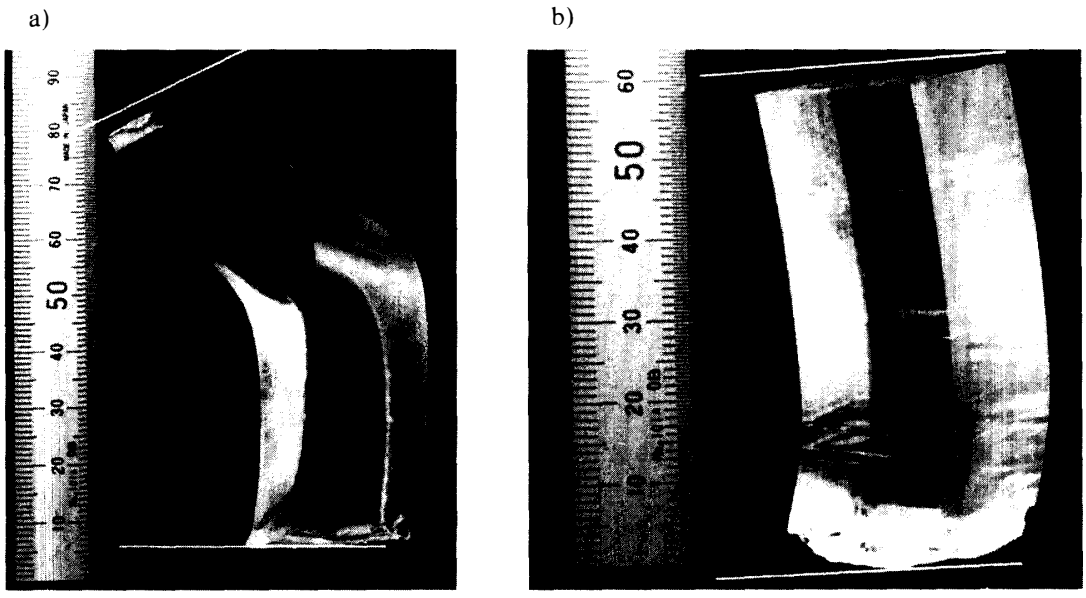


(Sample No. 2) (Sample No. 4)

*Fig. 5. Typical sample shapes after the compression test. a) is an example of no crack formation; b) is an example of crack along the basal plane.*

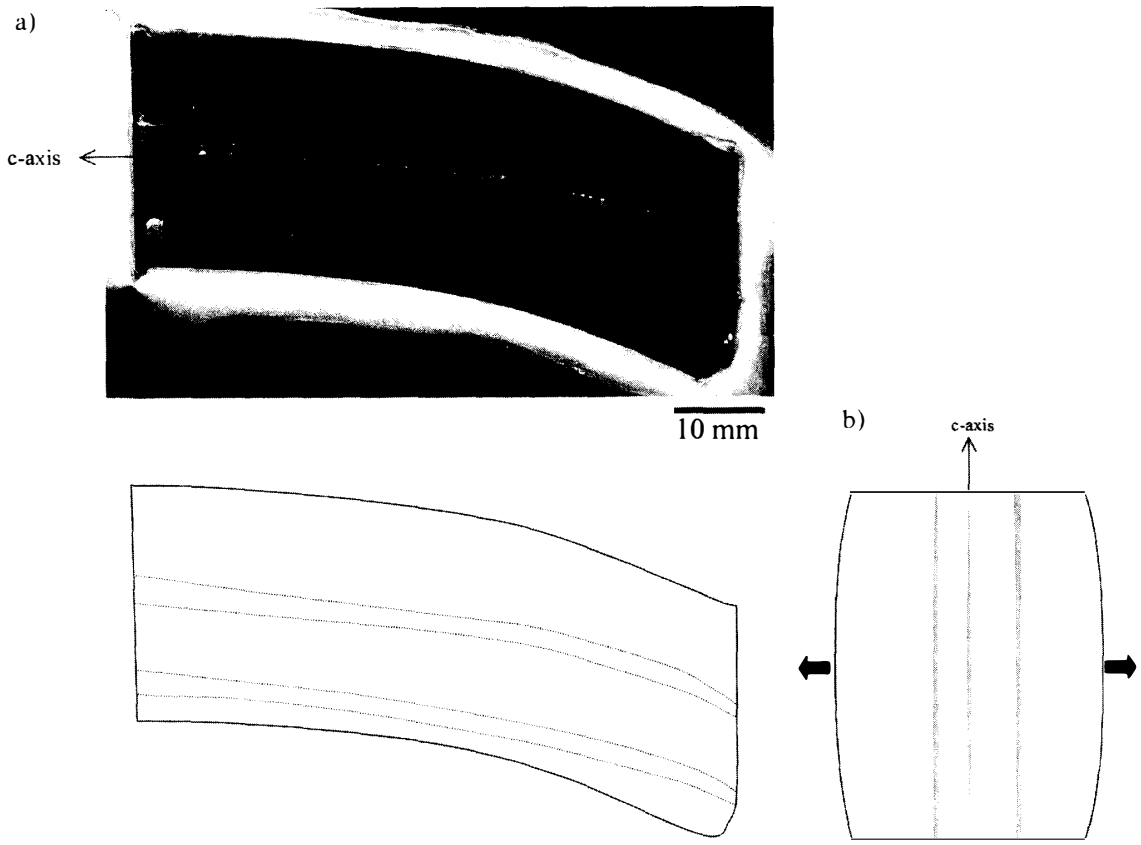


*Fig. 6.* *a) The upper photo is a thin section of sample No. 9; the lower sketch shows the crack distribution. In the lower sketch, dotted lines represent cracks along a prism plane. No cracks along the basal plane were observed in sample No. 9.*
*b) The formation and propagation mechanism of cracks along the plane parallel to the c-axis.*

variety of orientations. They reported that cracks grew along a $(10\bar{1}0)$ plane when the compression axis was inclined 5° from the *c*-axis. In this study, we observed that cracks grew along a parallel plane to the *c*-axis, which did not necessarily correspond to a lattice plane in addition to a $(10\bar{1}0)$ plane by etch pit observation.

2b) Cracks grew mostly along basal planes, but some cracks grew along the pane parallel to the *c*-axis (Fig. 5b, 7a). This pattern was observed only during the hydrostatic pressure experiment. In this condition, expanding in the horizontal direction is restricted remarkably by hydrostatic pressure. The vertical strain is caused by slight bending (Fig. 5b). This is almost the same condition as the three-point bending test of Nakaya (1958). Shear stress is applied along the basal plane in this experimental condition. Here, without rotation of the *c*-axis as observed in type 1 samples, a large shear stress is applied along the basal plane, and cracks grow along the basal plane (Fig. 7b).

During ice core drilling, there is only uniform deformation (*i.e.* no deformation such as bending) under the drill tip because the deformation area is surrounded by ice. Therefore, the above-mentioned crack formation type 2b probably best approximates the actual conditions of ice cutting just under the drill tip. These cracks have a great influence

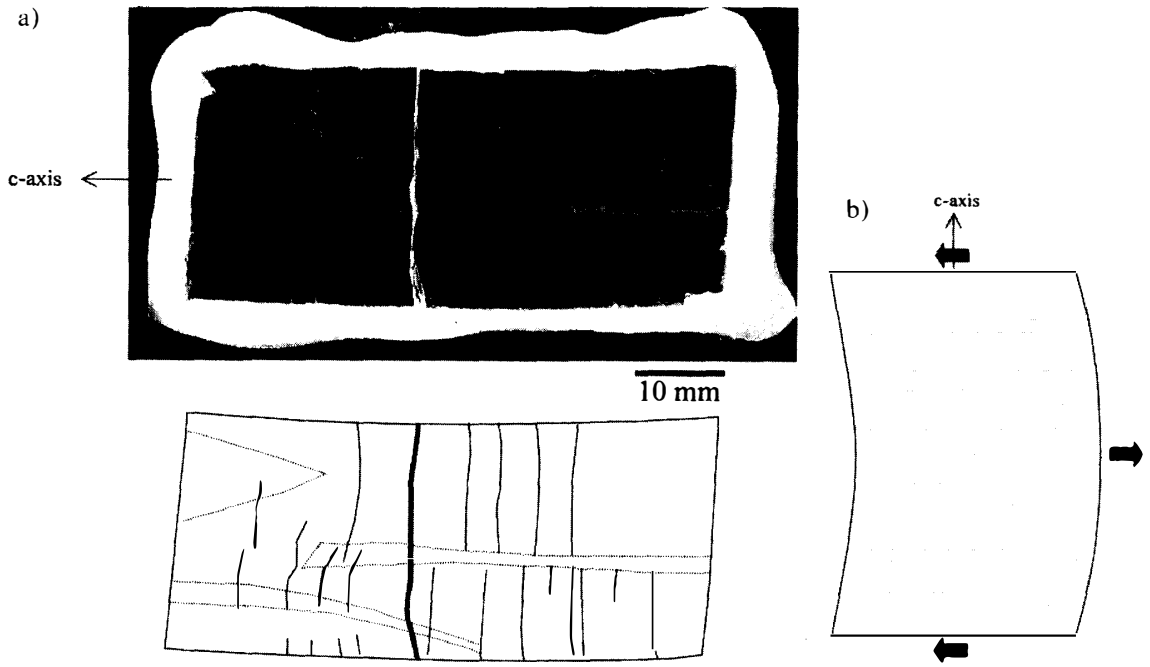


*Fig. 7.* *a) The upper photo is a thin section of sample No. 3; the lower sketch shows the crack distribution. In the lower sketch, solid lines represent cracks along a basal plane, whereas dotted lines represent cracks along a prism plane.*
*b) The formation and propagation mechanism of cracks along the plane parallel to the c-axis.*

on the chip size, drill pitch, and the difficulty of cutting the ice because the cutter removes ice with cracks.

## 4. Conclusions

Uniaxial compression tests were performed on ice single crystals at −18°C. The *c*-axis orientation of the test samples was aligned parallel to the compression axis. It was found that the test samples deformed by bending, twisting and crack formation probably caused by discrepancies in the angle between the stress axis and *c*-axis in this stress configuration. The sample with no cracks deformed non-uniformly, with bending and twisting, under both ambient pressure and hydrostatic pressure. Cracks grew only along planes parallel to the *c*-axis and basal plane. In compression tests under ambient pressure, cracks grew along planes parallel to the *c*-axis; but when the tests had a hydrostatic pressure of 20 MPa, cracks grew mostly along basal planes. It was estimated that cracks form at a critical stress at 15 MPa. With a stress level of over 15 MPa, cracks grew along the plane parallel to the *c*-axis and/or basal plane, depending on the direction of the stress axis. These conditions are thought to be realized under the drill tip of the cutter during ice core drilling. Crack-free ice cores might be recovered by adjusting the rotation speed of the drill, the rake angle of the cutter, and other quantities corresponding to the *c*-axis orientation. This study proposes that though ice cutting is basically a shearing process, it is important to understand that there are also compression processes in the vicinity of the cutter tip.

## Acknowledgments

This work was supported by a grant-in-aid for JSPS Fellows from the Japan Society for the Promotion of Science and a grant-in-aid for Scientific Research from the Ministry of Education, Science, Sports and Culture, Japanese Government.

## References

Higashi, A., Koinuma, S. and Mae, S. (1964): Plastic yielding ice single crystals. Jpn. J. Appl. Phys., **3**, 610-616.

Jones, S.J. and Brunet, J-G. (1978): Deformation of ice single crystals close to the melting point. J. Glaciol., **21**, 445-455.

Jones, S.J. and Glen, J.W. (1969): The mechanical properties of single crystals of pure ice. J. Glaciol., **8**, 463-473.

Nakaya, U. (1958): Mechanical properties of single crystals of ice. Part 1. Geometry of deformation. SIPRE Res. Rep., **28**.

Trickett, Y.L., Baker, I. and Pradhan, P.M.S. (2000): The orientation dependence of the strength of ice single crystal. J. Glaciol., **46**, 41-44.

*(Received February 14, 2001; Revised manuscript accepted September 10, 2001)*